Preparation and Characterization of Polyimide/Silane Coupling Agent Modified Multiwall Carbon Nanotubes Composites

Yao-Yi Cheng, Shang-Chih Chou, Jhih-Hong Huang

Institute of Organic and Polymeric Materials, National Taipei University of Technology, Taipei, 106, Taiwan

Received 1 November 2010; accepted 6 June 2011
DOI 10.1002/app.35041
Published online 12 October 2011 in Wiley Online Library (wileyonlinelibrary.com).

ABSTRACT: Polymer/carbon nanotube (CNT) nanocomposites have received much attention recently. In this study, we attempt to enhance the electrical conductivity of polyimide (PI) by variously modifying multiwall carbon nanotube (MWNT). We report the successful synthesis of PI/MWNT composite films using a blending process, and examine their properties and morphology. We modified MWNT by three different methods: thermal purification (U-CNT), oxidation with HNO_3 (N-CNT) and modification with a silane coupling agent (G-CNT). We confirmed the successful preparation of the modified MWNTs by Fourier transform infrared (FTIR) and Raman spectroscopy, and transmission electron microscopy (TEM). The low amorphous surface characteristics of N-CNT produced low surface resistance in the range of 10^5–10^6 Ω/cm^2 for the PI/N-CNT composites, which dispersed the buildup of electrostatic charge and improved dispersion. On the other hand, the better miscibility and interaction between G-CNT and PI, for the PI/G-CNT composites present superior thermal stability and mechanical properties. © 2011 Wiley Periodicals, Inc. J Appl Polym Sci 124: 1137–1143, 2012

Key words: polyimide; multiwall carbon nanotube; nanocomposite; coupling agent

INTRODUCTION

Carbon nanotubes (CNT) have excellent strength, elastic modulus, and electrical and thermal conductivity properties due to their intrinsic high aspect ratio (*L/D*) structure.[1] CNT have a wide variety of applications such as hydrogen storage,[2] chemical sensor,[3] nanoelectronic devices,[4] and flat-panel field emission displays.[5] They are potentially useful as nanoreinforcements in composite materials by the addition of small quantities into polymer materials. The potential role for CNTs in nanocomposites has attracted much attention recently.[6–9] Polymer/CNT nanocomposites properties depend on the dispersion and compatibility of CNT in the polymer matrix. The lack of interfacial interactions between CNT and the polymer matrix result in intrinsic strong van der waals interaction between CNTs, which causes their facile aggregation. To enhance the dispersion within a polymer matrix, it is necessary to modify CNT structure to place a polar functionality on the surface.[10–13] Many studies arm to disrupt CNT accretion, and improve dispersion by surface modification techniques such as chemical grafting-modification,[14–18] use of silane coupling agents,[19–21] ball milling,[22,23] and nonionic-surfactant modification.[24]

Correspondence to: Y.-Y. Cheng (ycheng@ntut.edu.tw).

Journal of Applied Polymer Science, Vol. 124, 1137–1143 (2012)

Polyimide (PI) is ubiquitous in the electronic and aerospace industries, due to its excellent mechanical properties, superior thermal stability, and chemical resistance. Reduction of PI electrical resistance lessens the build-up of electrostatic charge on the PI surface. Researchers have reported reduction in surface resistance to the range of 10^5–10^8 Ω/cm^2 by the addition of singlewall carbon nanotubes (SWNT)[25–28] or multiwall carbon nanotube (MWNT) to PI composites.[29–32]

The network-like structure of dispersed CNT reduces the amount of CNT necessary to improve the properties of PI/MWNT nanocomposites. In this study, we investigated PI/MWNT nanocomposites with various MWNT surface treatment modifications to improve their dispersion in the PI matrix. Nitric acid pretreatment provides well-dispersed PI/MWNT nanocomposites without significantly damaging the properties of MWNTs. Additionally, we used silane coupling agent to increase the degree of interaction between PI and MWNT for further improvement in mechanical properties and thermal stability of the PI/MWNT nanocomposites.

EXPERIMENTAL

Materials

Pristine MWNT with diameter 10–30 nm and length 5–15 μm was fabricated by chemical vapor deposition (CVD) with 95% purity supplied by Nano Port

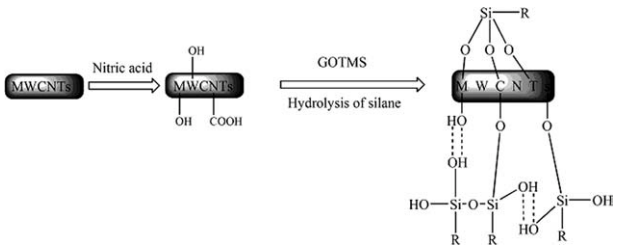

Figure 1 Schematic of silanization process of MWNT.

Corporation in China. 1-methyl-2-pyrrolodinone (NMP, Acros, 99%), nitric acid (HNO_3, Acros, 65%), γ-glycidyloxypropyltrimethylsilane (GOTMS, Acros, 97%), 3,3′,4,4′- biphenyl tetracarboxylic dianhydride (BPDA, CHRISKEV, 98%), and p-phenylenediamine (p-PDA, Acros, 99%), were used as received without further purification.

Preparation of nitric acid-modified MWNT

Pristine MWNT was purified by oxidation in air, at 550°C for 45 min, to remove amorphous carbon and residual metal catalyst to obtain the unmodified MWNT (U-CNT). After manual grinding by mortar for 10 min, U-CNT was mixed with 6*M* nitric acid using ultrasonication with power of 150W at room temperature for 30 min. The dispersed mixture was refluxed at 120°C for 3 h, washed, and filtered with distilled water and methanol, to obtain nitric acid-modified MWNT (N-CNT).

Preparation of silane-modified MWNT

N-CNT and γ-glycidyloxypropyltrimethylsilane, GOTMS (N-CNT:GOTMS = 1:1 by weight) were dispersed in distilled water by ultrasonication for 30 min, refluxed at 120°C for 6 h, and then washed and filtered with distilled water and methanol, to obtain silane-modified MWNT (G-CNT). Figure 1 shows a schematic of the silanization process.

Preparation of poly(amic acid) (PAA)

For the preparation of PI precursor, poly (amic acid), diamine p-PDA (0.05 mmol) was added to a flask and dissolved in NMP (73.5 g) with vigorous stirring. After 30 min, dianhydride BPDA (0.051 mmol) was added and reacted at room temperature under nitrogen for 4 h. The PAA solution was obtained with 12% wt % solid content. To control the molecular weight, the molar ratio of dianhydride and diamine was kept to 1.02:1.

Preparation of PAA/MWNT composites by blending

U-CNT, N-CNT, or G-CNT was added to NMP and ultrasonicated with power of 80 W at room temperature for 6 h to obtain a uniformly dispersed MWNT suspension, and then the solution was mixed with PAA. The mixture was stirred at room temperature under nitrogen for 12 h to obtain the PAA-MWNT composites. Figure 2 outlines the reaction scheme.

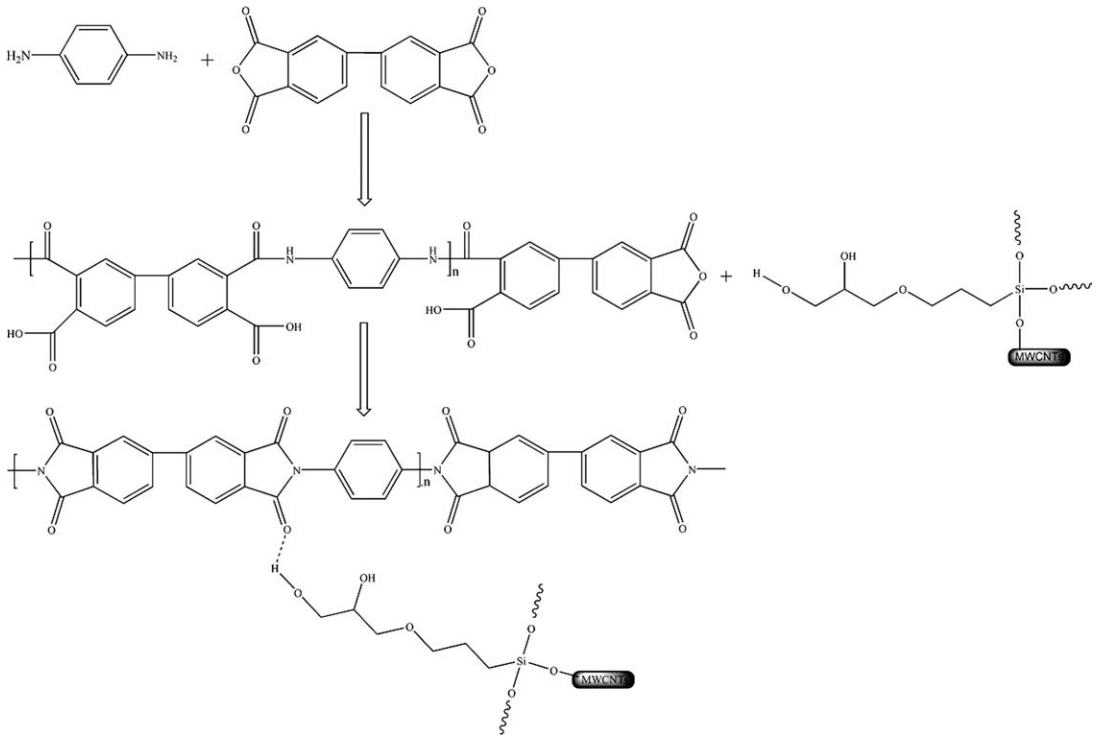

Figure 2 Reaction scheme for preparing PI/CNT composites.

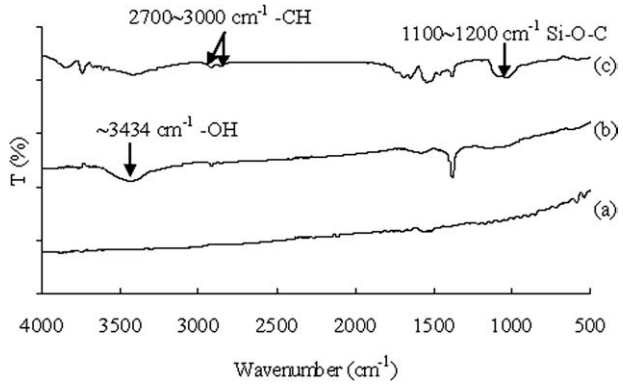

Figure 3 FTIR spectra of MWNTs: (a) U-CNT, (b) N-CNT, (c) G-CNT.

Synthesis of PI/MWNT hybrid films

The films were prepared by coating PAA solution on glass plates for multi-step thermal curing (100, 150, 200, 250, 300, and 400°C, each temperature held for 1 h) to provide the PI/MWNT films.

Characterization

FTIR analysis was performed with a Perkin-Elmer FTIR System. The JEOL-JEM-1230 microscope was used for transmission electron microscopy (TEM). Raman spectroscopy of powdered MWNT samples was performed using the Raman R-3000 over a scanning range of 200–2000 cm^{-1}, with an incident laser wavelength of 514 nm. To determine acid content of modified CNT, 0.2 g N-CNT or G-CNT was added into 100 mL of 0.01*N* NaOH, stirred for 24 h and

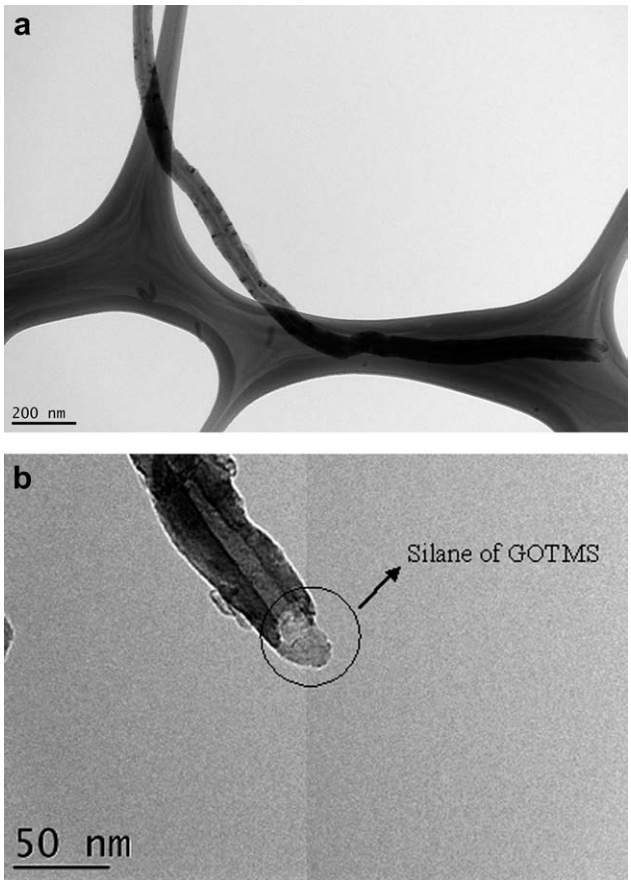

Figure 4 TEM image: (a) N-CNT, (b) G-CNT.

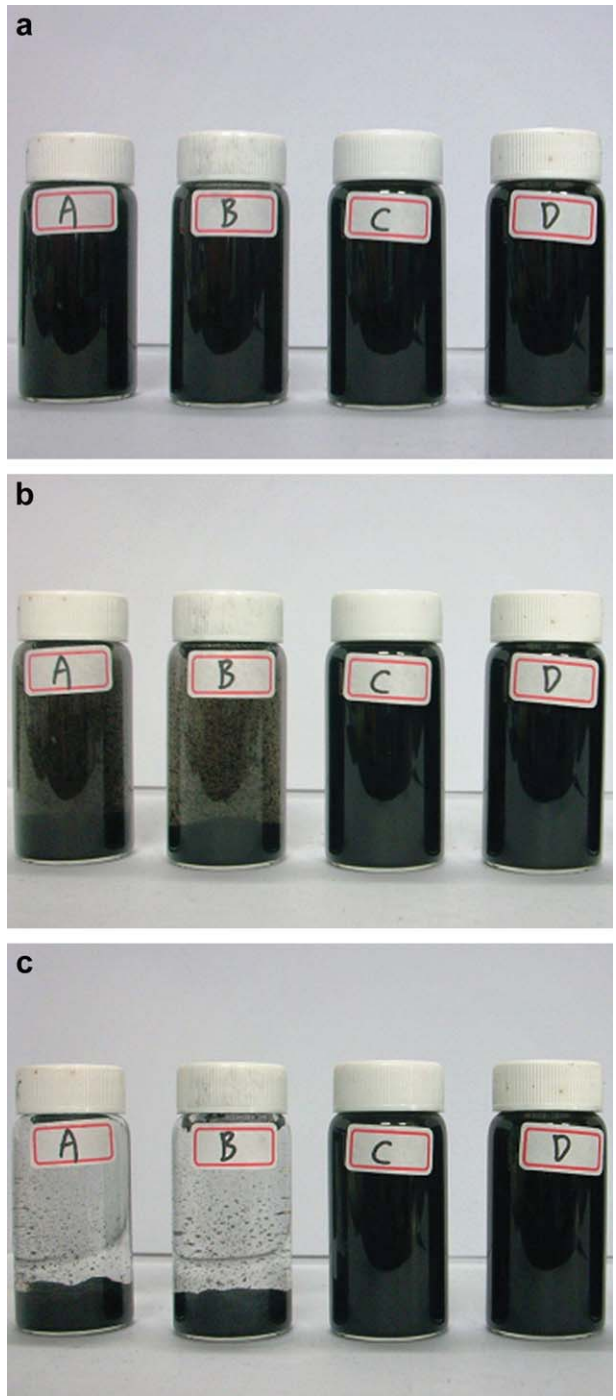

Figure 5 Dispersion states of MWNTs (A: untreated MWNT, B: U-CNT, C: N-CNT, D: G-CNT) after ultrasonication pretreatment for: (a) 10 min, (b) 1 h, (c) 1 week. [Color figure can be viewed in the online issue, which is available at wileyonlinelibrary.com.]

TABLE I
Characteristics of Various MWNTs

Sample	[a]T_{10} (°C)	[b]T_d (°C)	[c]R_s (%)	[d]G/D	[e]Electrical conductivity (S/cm)	Acid content (mmol/g)
U-CNT	528	594	1.8	1.2	3.1×10^{-1}	–
N-CNT	604	654	2	1.0	5.0×10^{0}	0.68
G-CNT	595	668	3.4	2.6	2.6×10^{0}	0.58

[a] T_{10}, 10% decomposition temperature.
[b] T_d, decomposition temperature at the maximum decomposition rate.
[c] Residues of TGA analysis at 900°C.
[d] *G*-band/*D*-band intensity ratio obtained by the integration of Raman curve.
[e] Electrical conductivity determined by four-probe method at room temperature.

then neutralized by titrating 0.01*N* HCl solution. Thermal gravimetric analysis (TGA) was performed with Netzsch TG 209 F3 equipment under nitrogen, from 35 to 900°C, with a heating rate of 20°C/min. Tensile testing was carried out with an Instron 4466 tester, at a tensile rate of 5 mm/min at room temperature. Five specimens (about 0.5 cm wide and 30 μm thick) were used for each PI composite. Electrical properties were measured with the ULTRA Mesohmeter SM-8200, and tests were conducted at room temperature, with voltage 100 V.

RESULTS AND DISCUSSION

Figure 3 compares the FTIR spectra of U-CNT, N-CNT, and G-CNT. As shown in trace (b), absorption bands at 3434 cm^{-1} for —OH group, 1720 cm^{-1} for C=O group and 1210 cm^{-1} for C—O group are present, suggesting that during the nitric acid treatment process, carboxylic acid, and hydroxyl groups formed most on the end of MWNT without significantly damaging the MWNT and reducing its length. TEM image of N-CNT is shown in Figure 4(a). In trace (c), the absorption band around 2700–3000 cm^{-1} represents an alkyl group stretch v(-CH), and the absorption band around 1100–1200 cm^{-1} results from the silane (Si—O—C) functional group, which confirms the successful reaction of GOTMS with MWNT to form G-CNT. The TEM image in Figure 4(b) shows silanized MWNT. Some amorphous silane molecules of GOTMS are present on the tube-end surface of a MWNT.

Figure 5 shows the dispersion states of untreated and modified MWNTs in distilled water at various time intervals. In Figure 5(a), all MWNTs show good dispersion after 10 min of ultrasonication. After 1 h, the untreated MWNT and U-CNT start to aggregate [Fig. 5(b)], which can be attributed to agglomeration due to their hydrophobic nature. The N-CNT and G-CNT samples in vials C and D, respectively, remained effectively dispersed because of their chemical surface treatments; these samples retained good suspension stability in distilled water even after one week [Fig. 5(c)].

The acid content of modified MWNT was determined by titration method, as summarized in Table I. After silane modification of N-CNT, the acid content is decreased from 0.68 mmol/g to 0.58 mmol/g, which is much less than the acid content of 2.55 mmol/g obtained for MWNT modified by mixed sulfuric and nitric acids (3:1 by volume) at 50°C for 2 h under ultrasonication. The thermal stability's of various modified MWNTs were examined by TGA. The U-CNT decomposition temperature at 10% weight loss and at the maximum decomposition rate is 528°C and 594°C, respectively; while N-CNT and

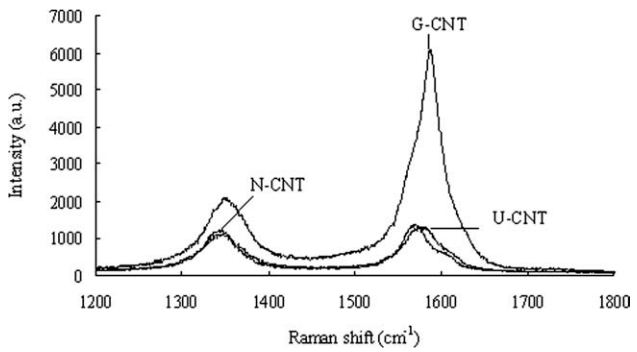

Figure 6 Raman spectra of various MWNTs.

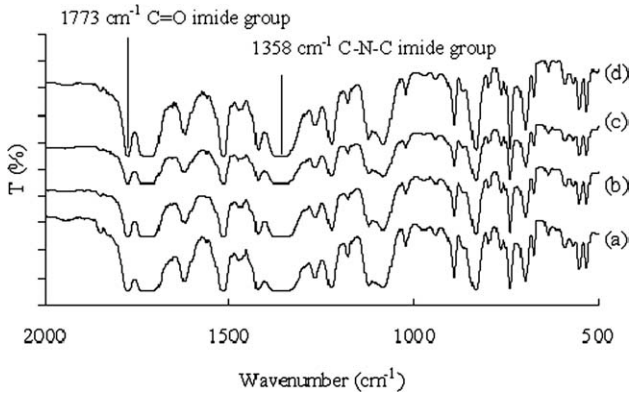

Figure 7 FTIR spectra: (a) PI and the PI hybrid films: (b) with U-CNT, (c) with N-CNT, (d) with G-CNT.

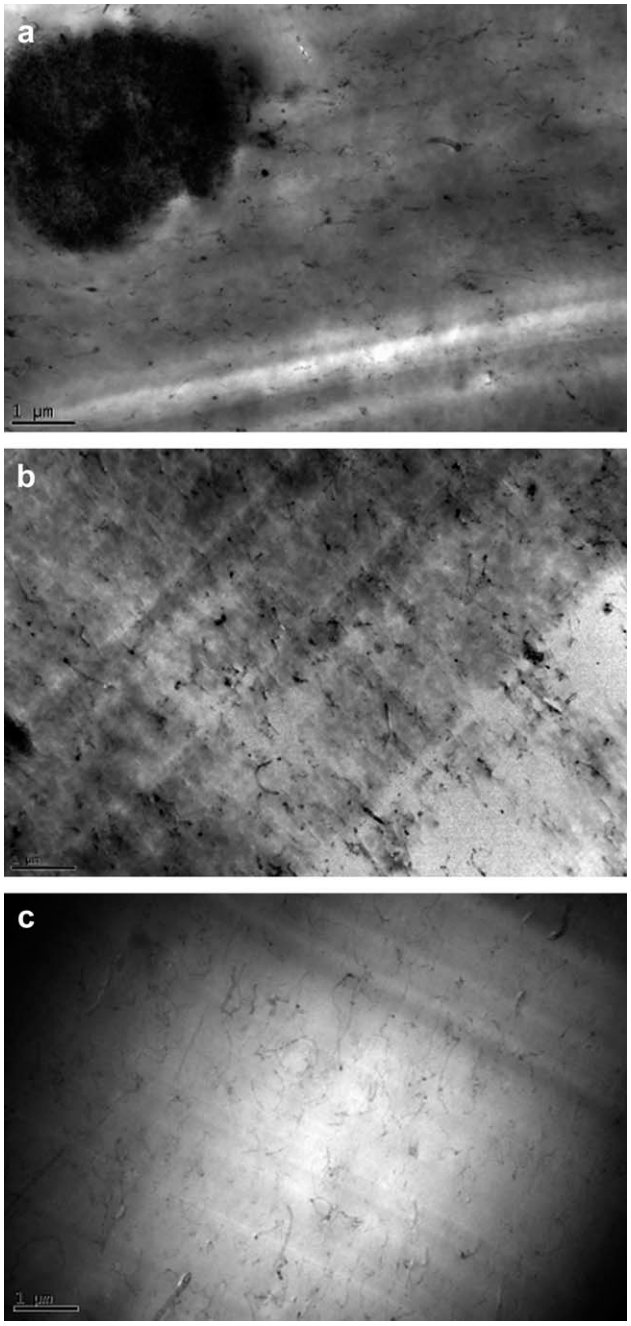

Figure 8 TEM images of the PI hybrid films: (a) with 3% U-CNT, (b) with 3% N-CNT, (c) with 3% G-CNT.

TABLE II
Thermal Properties of PI and PI/MWNT Composites

	10% decomposition temperature (°C)		
MWNT	ox-CNT	N-CNT	G-CNT
0%		598	
0.1%	601	599	616
0.5%	604	612	617
1%	609	612	621
2%	614	616	618
3%	620	616	625

TABLE III
Mechanical Properties of PI and PI/MWNT Composites

	Tensile Strength (MPa)			Elongation (%)			Young's modules (MPa)		
MWNT	ox-CNT	N-CNT	G-CNT	ox-CNT	N-CNT	G-CNT	Ox-CNT	N-CNT	G-CNT
0%		114.7 ± 16.7			3.7 ± 0.5			3.3 ± 0.5	
0.1%	121.4 ± 23.2	131.3 ± 21.7	160.1 ± 22.4	3.8 ± 1.8	2.7 ± 0.4	8.4 ± 1.0	4.0 ± 2.3	4.7 ± 0.9	2.6 ± 0.8
0.5%	127.3 ± 22.3	140.2 ± 17.9	162.8 ± 22.9	3.3 ± 2.0	5.2 ± 0.9	8.5 ± 4.2	5.6 ± 3.6	3.6 ± 0.5	2.6 ± 1.0
1%	128.2 ± 27.8	134.0 ± 33.7	181.3 ± 13.0	5.5 ± 1.5	5.5 ± 1.9	7.6 ± 0.4	3.0 ± 0.8	3.6 ± 1.0	2.8 ± 0.6
2%	138.7 ± 28.4	136.3 ± 25.3	172.7 ± 17.4	3.9 ± 0.3	3.1 ± 0.9	6.1 ± 1.1	4.0 ± 0.8	4.5 ± 0.6	3.1 ± 0.4
3%	138.3 ± 10.9	138.3 ± 22.9	136.3 ± 19.2	4.7 ± 1.1	4.8 ± 0.5	5.7 ± 1.0	3.6 ± 0.9	3.2 ± 1.5	3.0 ± 0.5

TABLE IV
Electrical Properties of PI and PI/MWNT Composites

	Surface resistance (Ω/cm^2)			Volume resistance (Ω-cm)		
MWNT	ox-CNT	N-CNT	G-CNT	ox-CNT	N-CNT	G-CNT
0%		4.5×10^{14}			3.6×10^{13}	
0.1%	2.5×10^{14}	4.2×10^{11}	1.2×10^{13}	8.3×10^{12}	1.5×10^{13}	1.2×10^{13}
0.5%	7.5×10^{13}	1.6×10^{11}	3.2×10^{13}	3.5×10^{10}	9.1×10^{10}	7.1×10^{12}
1%	6.2×10^{6}	2.9×10^{7}	7.3×10^{10}	8.3×10^{6}	1.2×10^{6}	3.5×10^{11}
2%	3.1×10^{6}	9.4×10^{5}	2.9×10^{10}	2.5×10^{6}	6.9×10^{5}	6.6×10^{8}
3%	3.5×10^{6}	2.9×10^{5}	1.6×10^{7}	3.3×10^{6}	3.1×10^{5}	5.6×10^{7}

G-CNT samples show enhanced thermal stabilities, as listed in Table I. Purified N-CNT can achieve better thermal stability under nitrogen and electrical conductivity than U-CNT, which suggests that the nitric acid treatment can effectively remove the remaining amorphous carbon of U-CNT. Table I also shows the *G/D* ratio obtained from Raman spectra shown in Figure 6. This indicates the degree of MWNT dispersion. G-CNT presents the highest *G/D* ratio because of a significant increase in the intensity of its G-band intensity. This suggests that using the GOTMS silane-coupling agents leads to significant improvement in MWNT dispersion above that of U-CNT and N-CNT.

For the preparation of PI films, a two-step procedure is commonly used. First, by the ring opening polyaddition of aromatic dianhydride and diamine in polar aprotic solution, a PAA solution is formed, in which MWNT can be uniformly dispersed. By thermal cyclodehydration processes, PAA/MWNT can be then converted to PI/MWNT films. Figure 7 compares the FTIR spectra of PI and PI/MWNT hybrid films. The conversion of PAA to PI can be elucidated by the decrease of the carbonyl acid absorption at 1672 cm^{-1}, and by the characteristic absorption bands of imide group observed at 1773 cm^{-1} (C═O asymmetric stretching), 1703 cm^{-1} (C═O symmetric stretching) and 1358 cm^{-1} (C─N─C imide ring stretching). The addition of these modified MWNTs into the PI matrix does not change the chemical structure of PI. Figure 2 presents the interaction between PI and silanol in G-CNT. However, there might be also reaction between unreacted carboxyl acid and the silanol, which can also improve the dispersion of G-CNT in the PI composites. In the TEM images shown in Figure 8(a), aggregation of bundled U-CNT is apparent, revealing the poor interaction between U-CNT and the PI matrix. As shown in Figure 8(b,c), purified N-CNT has better dispersion than U-CNT does, while G-CNT has the best dispersion and compatibility in the PI matrix.

Table II provides TGA thermal stability results of PI/MWNT nanocomposite films. The decomposition temperature (T_d) at 10% weight loss of pristine PI is 598°C. The PI/MWNT composite T_d increases gradually on addition of modified MWNT, which helps protect the PI composite film from thermal decomposition. T_d reaches a maximum temperature of 620°C for 3 wt % U-CNT added to the PI composite. Higher thermal decomposition temperatures are achievable by the addition of G-CNT into PI in place of either U-CNT or N-CNT, due to a more homogeneous dispersion of G-CNT, and stronger interaction with the PI matrix. The thermal decomposition temperature increases up to 625°C when the PI composite is combined with 3 wt% G-CNT.

Table III summarizes the tensile strength and elongation at break point for the PI nanocomposite films with various modified MWNT loadings. Formation of a network structure between MWNT and PI reduces the mobility of PI molecules, thereby increasing the strength of PI nanocomposite materials. G-CNT substituted PI produces nanocomposites with better tensile strength and elongation properties compared with U-CNT and N-CNT substitution. For 3 wt % U-CNT and N-CNT substituted PI samples, the tensile strength is about 138 MPa. On the other hand, the tensile strength of G-CNT samples reached a maximum of 181 MPa for 1 wt % G-CNT, about 1.5 times of that of PI. Better dispersion and stronger interaction occurs because of hydrogen bonding between the G-CNT and the PI matrix. This composition provides for better elasticity modulus without significant sacrifice of elongation of the PI nanocomposites.

MWNT's high aspect ratio of significantly improves electrical conductivity of the polymer matrix, enabling a reduction in surface electrostatic charge (ESC) buildup. Table IV shows that surface and volume resistances gradually decrease as MWNT content is increased. The criterion for electrostatic charge mitigation (10^6–10^8 Ω/cm^2) is met when PI is loaded with 1 wt% of U-CNT or N-CNT. However, 3 wt % of G-CNT is required for PI nanocomposites to meet the same criterion. This might be because of formation of an amorphous phase on the surface of G-CNT, which hinders MWNT electrical transportation in PI composites. Similarly, the formation of N-CNT using oxidative nitric acid produced a less amorphous surface, dispersion forms conductive paths, and increases electrical conductivity of

the PI nanocomposites. As the N-CNT loading reaches 3 wt %, PI nanocomposite electrical resistance reduces to $2.9 \times 10^5\ \Omega/cm^2$.

CONCLUSIONS

This study succeeded in fabricating a homogeneously dispersed PI nanocomposite with variously modified MWNTs. The MWNTs were modified in nitric acid to render a less amorphous surface, improve dispersion throughout the PI, and form effective conductive paths, thereby improving the electrical conductivity of the PI nanocomposite. Following treatment with a GOTMS silane coupling agent, the MWNTs were better able to disperse, thereby providing stronger PI matrix interactions, and significantly enhancing the mechanical and thermal properties of the nanocomposite.

References

1. Iijima, S. Nature 1991, 354, 56.
2. Lee, S. M.; Lee, Y. H. Appl Phys Lett 2001, 76, 2877.
3. Kong, J.; Franklin, N. R.; Zhou, C. W. Science 2000, 287, 622.
4. Avouris, P.; Hertel, T.; Martel, R.; Schmidt, T.; Shea, H. R.; Walkup, R. E. Appl Surf Sci 1999, 141, 201.
5. Chatelain, A.; Ugarte, D. A. Science 1995, 270, 1179.
6. Ma, P. C.; Tang, B. Z.; Kim, J. K. Carbon 2008, 46, 1497.
7. Shigeta, M.; Komatsu, M.; Nakashima, N. Chem Phys Lett 2006, 418, 115.
8. Wescott, J. T.; Kung, P.; Maiti, A. Appl Phys Lett 2007, 90, 033116.
9. Naeb, M.; Wang, J.; Xue, Y.; Wang, X.; Lin, T. J Appl Polym Sci 2010, 118, 359.
10. Bauhofer, W.; Kovacs, J. Z. Comp Sci Technol 2009, 69, 1486.
11. Du, F.; Scogna, R. C.; Zhou, W.; Brand, S.; Fischer, J. E.; Winey, K. I. Macromolecules 2004, 37, 9048.
12. Chiu, W. M.; Chang, Y. A. J Appl Polym Sci 2008, 107, 1655.
13. Gorga, R. E.; Lau, K. K. S.; Gleason, K. K.; Cohen, R. E. J Appl Polym Sci 2006, 102, 1413.
14. Zhou, B.; Lin, Y.; Hill, D. E.; Wang, W.; Veca, L. M.; Qu, L.; Pathak, P.; Meziani, M. J.; Diaz, J.; Connell, J. W.; Watson, K. A.; Allard, L. F.;Sun Y. P. Polymer 2006, 47, 5323.
15. Lin, Y.; Rao, A. M.; Sadanadan, B.; Kenik, E. A.; Sun, Y. P. J Phys Chem B 2002, 106, 1294.
16. Koos, A. A.; Horvath, Z. E.; Osvath, Z.; Tapaszto, L.; Niesz, K.; Konya, Z.; Kiricsi, I.; Grobert, N.; Ruhle, M.; Biro, L. P. Mater Sci Eng C 2003, 23, 1007.
17. Kim, J. A.; Seong, D. G.; Hang, T. J.; Youn, J. R. Carbon 2006, 44, 1898.
18. Hu, Y.; Wu, L.; Shen, J.; Ye, M. J Appl Polym Sci 2008, 110, 701.
19. Chen, H.; Jacobs, O.; Wu, W.; Rudiger, G.; Schadel, B. Polym Test 2007, 26, 351.
20. Ma, P. H.; Kim, J. A.; Tang, B. Z. Carbon 2006, 44, 3232.
21. Ma, P. H.; Kim, J. A.; Tang, B. Z. Comp Sci Technol 2007, 67, 2965.
22. Liu, F.; Zhang, X.; Cheng, J.; Tu, J.; Kong, F.; Huang, W.; Chen, C. Carbon 2003, 41, 2527.
23. Ma, P. H.; Tang, B. Z.; Kim, J. K. Chem Phys Lett 2008, 458, 166.
24. Jodgire, P. V.; Bhattacharyya, A. R.; Bose, S.; Gupta, N.; Kulkarni, A. R.; Misra, A. Chem Phys Lett 2006, 432, 480.
25. Smith, J. G.; Connell, J. W.; Delozier, D. M.; Lollehei, P. T.; Watson, K. A.; Lin, Y.; Zhou, B.; Sun, Y. P. Polymer 2004, 45, 825.
26. Smith, J. G.; Delozier, D. M.; Connell, J. W.; Watson, K. A. Polymer 2004, 45, 6133.
27. Yu, A.; Hu, H.; Bekyarova, E.; Itkis, M. E.; Gao, J.; Zhao, B.; Haddon, R. C. Comp Sci Technol 2006, 66, 1187.
28. Delozier, D. M.; Watson, K. A.; Smith, J. G.; Connell, J. W. Comp Sci Technol 2005, 65, 749.
29. So, H. H.; Cho, J. W.; Sahoo, N. G. Eur Polym J 2007, 43, 3750.
30. Zhu, B. K.; Xie, S. H.; Xu, Z. K.; Xu, Y. Y. Comp Sci Technol 2006, 66, 548.
31. Yuen, S. M.; Ma, C. C.; Chiang, C. L.; Lin, Y. Y.; Teng, C. C. J Polym Sci Part A: Polym Chem 2007, 45, 3349.
32. Wu, K. L.; Chou, S. C.; Cheng, Y. Y. J Appl Polym Sci 2010, 116, 3111.